Available online at www.sciencedirect.com
SCIENCE DIRECT®
Journal of Chromatography A, 1088 (2005) 1–15
JOURNAL OF CHROMATOGRAPHY A
www.elsevier.com/locate/chroma

Chromatographic classification and comparison of commercially available reversed-phase liquid chromatographic columns containing polar embedded groups/amino endcappings using principal component analysis

Melvin R. Euerby[a,*], Patrik Petersson[b]

[a] *AstraZeneca R&D Charnwood, Analytical Development, Pharmaceutical and Analytical R&D–Charnwood/Lund, Bakewell Road, Loughborough, Leicestershire LE11 5RH, UK*
[b] *AstraZeneca R&D Lund, Analytical Development, Pharmaceutical and Analytical R&D—Charnwood/Lund, Lund S-22187, Sweden*

Available online 13 November 2004

Abstract

Polar embedded phases have become increasingly popular in liquid chromatography (LC) analysis. These phases can produce diverse chromatographic selectivities as a result of their differing base silica, the type of polar embedded group (i.e. amide, urea, carbamate, ether or sulphonamide moieties) and the length of the alkyl ligand. Four column characterization protocols, using differing test probes, have been used to characterize 18 of these phases together with 17 alkyl phases (some of which contained novel polar endcapping, i.e. amino), which have been evaluated using principal component analysis (PCA). PCA provided graphical comparisons of the differences/similarities between these phases and between their corresponding C-alkyl, amino endcapped and enhanced polar selectivity phases.

Keywords: Stationary phases, LC; Column characterization; Polar embedded phases; Amino endcapped phases; Principal component analysis

1. Introduction

The number and diversity of commercially available reversed phase liquid chromatography (RPLC) stationary phases that contain a polar embedded (PEG) functionality has increased dramatically [1].

Their popularity within the chromatographic fraternity is due to their:

(i) Improved peak shape of basic analytes as a result of their decreased interaction with the phase's silanol groups, which may be attributed to the phase's silanol groups preferentially hydrogen bonding with the embedded functionality instead of the basic analytes [2–7]. It is also feasible that some of these phases contain a positive charge (i.e. residual amino functionality or a positive charge residing on the carbamate moiety) which results in repulsion of the protonated bases away from the silica surface.
(ii) Differing separation selectivities may be exhibited compared to standard C_{18} or C_8 phases, this is especially relevant when mixtures of bases, acids and neutrals are analysed [2–4,9–12]. This is due to the possible repulsion or attraction of bases and acids due to electrostatic interactions between the phase and the analytes. In addition, PEG phases have been observed to possess enhanced retention of phenolic compounds (i.e. hydrogen donors) as a result of their hydrogen bonding capacity [13].
(iii) Decreased hydrophobic character as a result of the incorporation of a polar functionality into the alkyl ligand [2–4].
(iv) Increased wettability of these phases affords the opportunity to use them in conjunction with high aqueous containing mobile phases without the mobile phase

* Corresponding author. Tel.: +44 1509 64 4084; fax: +44 1509 64 5590.
E-mail address: mel.euerby@astrazeneca.com (M.R. Euerby).

0021-9673/$ – see front matter © 2004 Elsevier B.V. All rights reserved.
doi:10.1016/j.chroma.2004.10.027

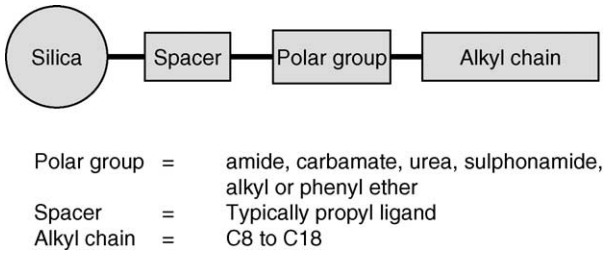

Fig. 1. Schematic representation of a typical polar embedded phase.

being driven out of the pores due to surface tension effects—producing "phase collapse or chain folding" if the flow/pressure is too low [14,15]. Hence, the phases are favoured for the RP analysis of very polar analytes requiring 100% aqueous mobile phase conditions.

The structure of the polar embedded phases (PEG) is typified in the schematic diagram shown in Fig. 1; where the spacer grouping is usually a propyl moiety between the silica surface and the polar grouping. The latter can be quite diverse in chemical functionality (i.e. amide, carbamate, urea, sulphonamide, alkyl ether, phenyl ether moieties). The C-alkyl ligand, which provides the lipophilic character to the phase, can vary in chain length from C_8 to C_{18}.

Traditionally, the nitrogen containing PEG phases were prepared from pre-formed aminopropyl silica [16–18]. For example, the *N*-acylaminopropyl bonded phases, more commonly known as the amide type PEG phases, are produced from the reaction of the appropriate aminopropyl silica with a suitable acid chloride [16]. This is known as a two-step synthesis (i.e. silica → aminopropyl silica → PEG phase), and as a consequence of steric hindrance, complete acylation is impossible. Therefore, a large and varied amount of unreacted amino groups will be present on the phase, which generates potential anionic exchange sites [19]. More recently, nitrogen containing PEG phases have been made using a one-step synthesis which bonds the pre-formed PEG containing silylating ligands directly onto the base silica, thus eliminating the presence of anionic sites [4,20].

Unfortunately, not all manufacturers are willing to divulge the functionality, bonding technology and composition of their commercially available stationary phase column chemistries. The PEG functionality and the bonding technology employed in their preparation will, undoubtedly, result in the production of nominally similar type phases possessing wildly differing chromatographic properties.

The paper describes the use of the chemometric tool principal component analysis (PCA) in order to assess the chromatographic similarity/dissimilarity of a range of commercially available PEG phases and compares them to their C-alkyl analogues and to a range of "Aqua" and amino endcapped phases. The chromatographic classification protocols of Neue [8], Tanaka [21,22] and Layne [2] have been used together with a newly developed testing routine to discriminate between these types of phases.

2. Experimental

2.1. Chemicals and reagents

All solvents used were of at least HPLC grade supplied by Romil (Cambridgeshire, UK) except for the water, which was provided by a Milli-Q-plus 185 ultra pure water system (Molsheim, France). Test analytes and mobile phase chemicals were supplied by Sigma–Aldrich (Dorset, UK) and Fisher Scientific (Leicestershire, UK).

The Tanaka column characterization procedure was performed as reported previously [21]. This protocol was additionally amended to assess for phenolic selectivity by the incorporation of benzyl alcohol (0.3 mg/ml in methanol–water, 1:1, v/v) into the ion exchange capacity testing.

The structure of the test analytes is given in Fig. 2.

Acid mixture 1 (modified from the Waters [23] and Laynes [2] published work) consisted of equal volumes of 4-hydroxybenzoic acid, sorbic acid, benzoic acid, 2-hydroxybenzoic acid, *trans*-cinnamic acid, 3-phenylpropionic acid, phenol, propyl paraben (all at 0.3 mg/ml in methanol–water 3:7, v/v) and dimethylphthalate (0.3 mg/ml in methanol–water, 1:1, v/v).

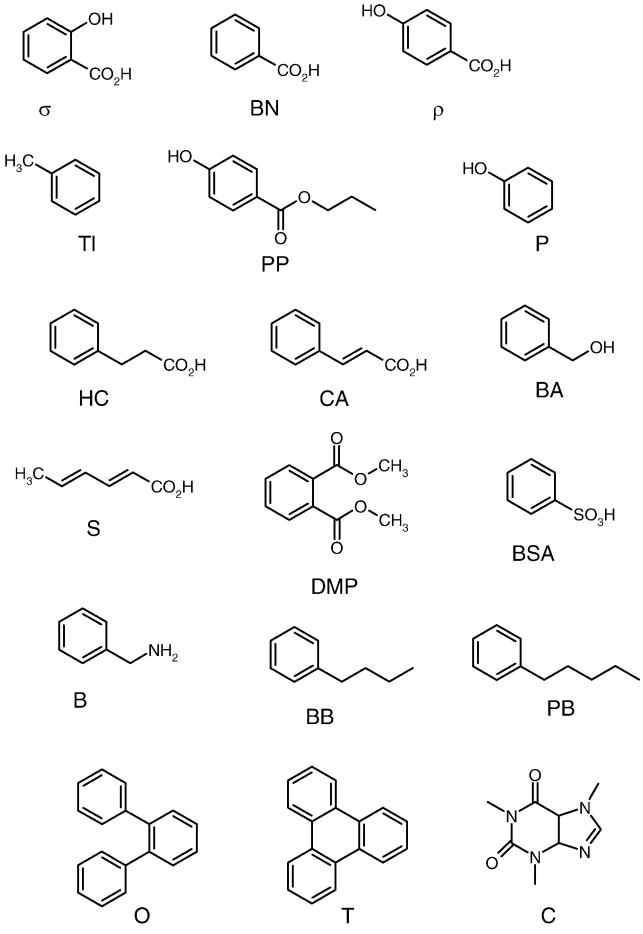

Fig. 2. Structure, code for the test analytes.

Acid mixture 2: equal volumes of toluene (0.3 mg/ml in methanol–water, 1:1, v/v/), benzylalcohol (0.3 mg/ml in methanol–water 1/4, v/v), phenol and benzene sulphonic acid (both 0.3 mg/ml in water).

2.1.1. Preparation of phosphoric acid/potassium dihydrogenphosphate buffer, pH 2.5 and 50 mM ionic strength

Phosphoric acid (2.414 g, 85%) and potassium dihydrogenphosphate (6.273 g) was dissolved in 800 ml of water and subsequently and made up to 1000 ml with water.

2.2. Instrumentation

HPLC separations were performed on an Agilent Technologies 1100 liquid chromatograph with ChemStation v. 9.03 LC software (Agilent Technologies, Cheadle, Cheshire) equipped with Agilent column/solvent selection valves.

2.3. Liquid chromatography

At least 20 column volumes of the appropriate mobile phase were flushed through the column prior to commencing the testing. All columns were new as supplied by the manufacturer/supplier. The columns characterized in this study are shown in Table 1.

The chromatographic conditions for the Tanaka HPLC characterization of the phases were as reported previously [21].

Acid mixtures 1 and 2 were chromatographed using a mobile phase composition of 5 mM phosphate buffer pH 2.5 in methanol–water (35:65 and 65:35, v/v, for acid mixtures 1 and 2, respectively). For example, to prepare 1000 ml of 35:56 (v/v) mobile phase—100 ml of 50 mM buffer was mixed with 550 ml of water and 350 ml of methanol.

The first disturbance of the baseline on the injection of methanol was used as dead time marker. For acid mixtures 1 and 2, a 10 μl injection volume and a 1 ml/min flow rate have been employed (for column dimensions other than 150 mm × 4.6 mm i.d. the injection volume and flow rate have been scaled appropriately). The analytes typically eluted within 60 min for all the tests.

The different chromatographic parameters used in the characterization procedures are briefly described below:

2.4. Tanaka protocol

2.4.1. Retention factor for n-pentylbenzene, k_{PB}

Reflects the surface area and surface coverage (ligand density).

2.4.2. Hydrophobicity or hydrophobic selectivity, α_{CH_2}

Retention factor ratio between *n*-pentylbenzene (PB) and *n*-butylbenzene (BB), $\alpha_{CH_2} = k_{PB}/k_{BB}$. This is a measure of the surface coverage of the phase as the selectivity between alkylbenzenes differentiated by one methylene group is dependent on the ligand density.

2.4.3. Shape selectivity, $\alpha_{T/O}$

Retention factor ratio between triphenylene (T) and *o*-terphenyl (O), $\alpha_{T/O} = k_T/k_O$. This descriptor is a measure of the shape selectivity, which is influenced by the spacing of the ligands and probably also the shape/functionality of the silylating reagent.

2.4.4. Hydrogen bonding capacity, $\alpha_{C/P}$

Retention factor ratio between caffeine (C) and phenol (P), $\alpha_{C/P} = k_C/k_P$. This descriptor is a measure of the number of available silanol groups and the degree of endcapping.

2.4.5. Total cation-exchange capacity, $\alpha_{B/P}$ pH 7.6

The retention factor ratio between benzylamine (B) and phenol, $\alpha_{B/P}$ pH 7.6 = k_B/k_P. This is an estimate of the total silanol activity.

2.4.6. Acidic cation-exchange capacity, $\alpha_{B/P}$ pH 2.7

The retention factor ratio between benzylamine and phenol, $\alpha_{B/P}$ pH 2.7 = k_B/k_P. This is a measure of the acidic activity of the silanol groups.

2.5. Acid mixtures 1 and 2

2.5.1. Phenolic selectivity, $\alpha_{P/DMP}$, $\alpha_{P/BA}$, $\alpha_{P/Tl}$

Retention factor ratio between phenol and dimethylphthalate (DMP), $\alpha_{P/DMP} = k_P/k_{DMP}$ (this test is analogous to that of butyl paraben and dipropylphthalate as described by Neue et al. [23]), phenol and benzyl alcohol (BA), $\alpha_{P/BA} = k_P/k_{BA}$ and phenol and toluene (Tl), $\alpha_{P/Tl} = k_P/k_{Tl}$. These are measures of the enhanced retention of phenol compared to non-phenolic analytes.

2.5.2. Hydrophobicity, $\alpha_{PP/P}$

Retention factor ratio between propyl paraben (PP) and phenol, $\alpha_{PP/P} = k_{PP}/k_P$. The difference in the retention of the two analytes corresponds to a *n*-propyl ester moiety.

2.5.3. Hydrophilicity, $\alpha_{BA/Tl}$

Retention factor ratio between benzyl alcohol and toluene, $\alpha_{BA/T} = k_{BA}/k_{Tl}$. This is a measure of the polarity of the phase.

2.5.4. Shape/steric selectivity, $\alpha_{CA/HC}$, $\alpha_{BN/S}$

Retention factor ratio between cinnamic acid (CA) and 3-phenylpropionic acid (HC), $\alpha_{CA/HC} = k_{CA}/k_{HC}$ and benzoic acid (BN) and sorbic acid (S), $\alpha_{BN/S} = k_{BN}/k_S$. This descriptor is a measure of the shape selectivity, which is influenced by the spacing of the ligands and probably also the shape/functionality of the silylating reagent.

2.5.5. Anion-exchange capacity, $\alpha_{\sigma/BN}$, $\alpha_{\sigma/\rho}$ $\alpha_{BSA/Tl}$

Retention factor ratio between 2-hydroxybenzoic acid (σ) and benzoic acid, $\alpha_{\sigma/BN} = k_\sigma/k_{BN}$; 2-hydroxybenzoic acid

Table 1
Columns characterized and manufacturers details

Column no.	Column	Supplier/producer	Linker silica to polar group	Type of polar embedded group	Ligand length	Comments	Pore size (nm)	Surface coverage ($\mu mol/m^2$)
1	XTerra MSC_8	Waters Ltd.	N/A	None	C_8	Trifunctional bonding + endcapped, 12% C load	12.4	2.35
2	XTerra RP8	Waters Ltd.	Propyl	Carbamate	C_8	Monofunctional bonding + endcapped, 13.5% C load	12.5	2.41
3	Prism RP	ThermoElectron	Not specified	Urea	C_{12}	Endcapped, 12% C load	10	3.1
4	BetaMax Acid	ThermoElectron	Not specified	Not specified	Long alkyl chain	Endcapped, 15% C load	6	
5	Polaris C_{18} A	Varian	Not specified	Not specified	Unknown C_{18}	Polar endcapped	18	
6	Polaris Amide C_{18}	Varian	Not specified	Amide	Amide C_{18}	Polar endcapped	18	
7	MetaSil Basic	Varian	N/A	None	Short chain alkyl groups	Monomeric bonding	10	
8	Synergi Polar-RP	Phenomenex	Not specified	Phenyl ether	C_8	Polar endcapping, 11 % C load	8	3.15
9	Symmetry C_8	Waters Ltd.	N/A	None	C_8	Endcapped, 11.7% C load	10	
10	Symmetry Shield RP8	Waters Ltd.	Propyl	Carbamate	C_8	Endcapped, 15% C load	10	3.29
11	HyPURITY C_8	ThermoElectron	N/A	None	C_8	Endcapped, 8% C load	18	
12	HyPURITY Advance	ThermoElectron	Propyl	Not specified	C_8	Not endcapped, 10% C load	18	
13	ZorbaxSB C_{18}	Agilent Tech.	N/A	None	C_{18} + di-isobutyl side groups on silyating group	Monomeric bonding + uncapped, 10% C load	8	2.98
14	Zorbax Bonus RP	Agilent Tech.	Propyl	Amide	C_{14}	Bulky steric protecting groups, triple endcapped, 10% C load	8	2.1
15	Nucleosil C_{18} HD	Macherey-Nagel	N/A	None	C_{18}	Endcapped, 20% C load	10	
16	Nucleosil Nautilus C_{18}	Macherey-Nagel	Not specified	Not specified	C_{18}	Endcapped, 16% C load	10	
17	Discovery C_{18}	Supelco	N/A	None	C_{18}	Monofunctional bonding + endcapped	18	3
18	Discovery RP amide C_{16}	Supelco	Propyl	Amide	C_{16}	Monofunctional bonding + endcapped	18	2.6
19	Purospher RP-18	Merck	N/A	None	C_{18}	Uncapped, 18% C load	8	
20	Thermo BS535	ThermoElectron	N/A	None	C_{18}	Amino endcapped		
21	Purospher RP-18e	Merck	N/A	None	C_{18}	Endcapped 18%, C load	12	
22	Symmetry C_{18}	Waters Ltd.	N/A	None	C_{18}	Endcapped, 19.1% C load	10	3.09
23	Symmetry Shield RP18	Waters Ltd.	Propyl	Carbamate	C_{18}	Endcapped, 15% C load	9	3.21
24	Polaris C_8 Ether	Varian	Not specified	Ether	C_8		18	
25	Polaris C_{18} Ether	Varian	Not specified	Ether	C_{18}		18	
26	HyPURITY Aquastar	ThermoElectron	N/A	None	C_{18}	Polar endcapped		
27	Atlantis dC_{18}	Waters Ltd.	N/A	None	C_{18}	Difunctionally bonded endcapped 12% C load	10	
28	Suplex pKb	Supelco	Not specified	Not specified	Not specified		10	
29	Lichropsher RP Select B	Merck	N/A	None	C_8	Endcapped, 12% C load	6	3.2
30	Supelcosil ABZ	Supelco	Propyl	Amide	C_{16}	Polymeric bonding + endcapping with methyl amide	12	
31	Synergi Max RP	Phenomenex	N/A	None	C_{12}	TMS endcapping, 17% C load	8	3.21
32	XTerra MSC_{18}	Waters Ltd.	N/A	None	C_{18}	Trifunctional bonding + endcapped, 15.5% C load	12.5	
33	XTerra RP18	Waters Ltd.	Propyl	Carbamate	C_{18}	Monofunctional bonding + endcapped, 15% C load	12.5	
34	HyPURITY C_{18}	ThermoElectron	N/A	None	C_{18}	Endcapped, 13% C load	18	
35	Acclaim PAC_{16}	Dionex	Propyl	Sulphonamide + ether linkage	C_{16}	Monofunctional bonding, endcapped, 17% C load	12	

and or 4-hydroxybenzoic acid (ρ), $\alpha_{\sigma/\rho} = k_\sigma/k_\rho$, and benzenesulphonic acid (BSA) and toluene, $\alpha_{BSA/Tl} = k_{BSA}/k_{Tl}$. These are measures of the anion exchange capacity of the phase as shown by the increased retention of the acidic analytes.

2.6. Software employed

2.6.1. Principal component analysis

PCA was performed using Simca-P 8.1 software (Umetrics, Sweden). In order to give all variables the same importance, the variables were "auto scaled", i.e. the average was subtracted from each variable and each variable was divided by its standard deviation.

2.6.2. log D and pK_a predictions

Predictions of pK_a and log D were calculated using Advanced Chemistry Development software programme version 6.0 (Toronto, Canada).

3. Results and discussion

3.1. Column characterization parameters

In contrast to standard C_{18} phases (for example see references [21–23,31–35]), there have been limited studies into the characterization and comparison of polar embedded phases [2,8,13,24]. It has been previously reported that acidic probes, such as maleic acid, 2-hydroxybenzoic acid and 5-ethylpyridinedicarboxlic acid, can highlight differences in hydrogen bonding capacity and/or any secondary interactions arising from ionic interactions with the phase [2,4,16,25]. The Waters selectivity factor for butyl paraben/dipropyl phthalate when plotted against the retention factor of acenaphthene has been shown to discriminate between classical alkyl phases and those incorporating polar groupings [8]. It is postulated that the enhanced retention of phenolic analytes such as butyl paraben (i.e. an H-bonding donor) may be attributed to the interaction of the phenolic proton and the highly polarized carbonyl oxygen of the polar embedded amide, urea and carbamate groupings [4,13].

We have utilized a modified column characterization protocol based on that described by Layne [2], the Waters group [8] and Tanaka [21,22] to characterize 18 commercially available PEG phases which contain a diverse range of polar functionality/alkyl chain lengths, 13 corresponding standard C-alkyl phases and four polar endcapped phases.

3.2. Acid mixture 1

Selected parameters from the chromatographic protocols of Neue [4,8,20,23] and Layne [2] were performed on 24 differing stationary phases including 15 containing polar embedded groups (i.e. amide, urea, phenyl ether sulphonamide and carbamate moieties), and nine standard alkyl phases (see Tables 1 and 2). Where possible, the polar embedded and corresponding alkyl phases bonded onto the same base silica were employed in the study, this was achieved with XTerra, Polaris, Symmetry, HyPURITY, Zorbax, Nucleosil and Discovery materials.

A low ionic strength (i.e. 5 mM PO_4 pH 2.5 in MeOH–water (35:65, v/v), 40 °C) containing mobile phase was employed to exacerbate any ionic interactions that the stationary phase may have with the anionic analytes.

The selectivity factors (α) for the following analyte pairs were calculated; $\alpha_{CA/HC}$, $\alpha_{BN/S}$, $\alpha_{\sigma/BN}$, $\alpha_{\sigma/\rho}$, $\alpha_{P/DMP}$, $\alpha_{PP/P}$ (see Table 2). An $\alpha_{BN/S}$ value of 1 was obtained for all the alkyl phases evaluated, whereas, without exception, all the PEG phases generated an $\alpha_{BN/S}$ value >1. In addition, the $\alpha_{CA/HC}$ value for the PEG phases was always greater than that for their corresponding C-alkyl analogues. Large $\alpha_{\sigma/BN}$, $\alpha_{\sigma/\rho}$ values were indicative of nitrogen containing PEG phases that possessed amino functionality on the phase; the most plausible explanation for this would be that these phases had been synthesed using a two-stage procedure. See Fig. 3A–D for a comparison of two manufacturers polar embedded phases against their C-alkyl analogues bonded onto the same base silica. The Advance material

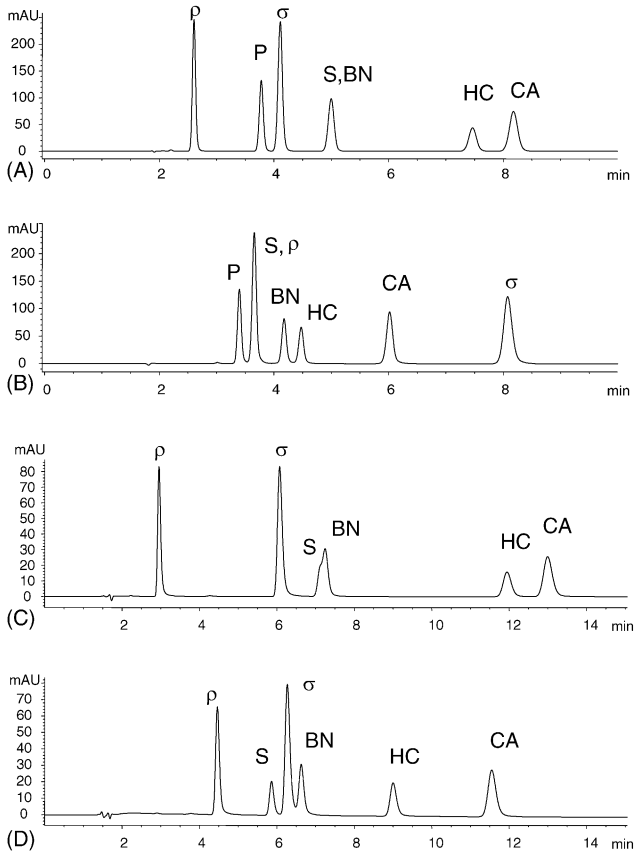

Fig. 3. Representative chromatograms of the acid mixture 1 using the phases: (A) HyPURITY C_8; (B) HyPURITY Advance; (C) Symmetry C_8; (D) Symmetry RP8 Shield. See Fig. 2 for peak assignments and Section 2 for chromatographic conditions.

Table 2
Column characterization results using the acid mixtures 1, 2, the Tanaka protocol plus Tanaka partial modification

Column no.	Column	Acid mixture 1						Acid mixture 2			
		$\alpha_{CA/HC}$	$\alpha_{BN/S}$	$\alpha_{\sigma/BN}$	$\alpha_{\sigma/\rho}$	$\alpha_{P/DMP}$	$\alpha_{PP/P}$	$\alpha_{BSA/TI}$	$\alpha_{P/BA}$	$\alpha_{P/TI}$	$\alpha_{BA/TI}$
1	XTerra MSC_8	1.27	1.00	0.76	3.01	0.30	9.47	0.00	1.00	0.17	0.17
2	XTerra RP8	1.48	1.18	1.001	1.68	0.55	7.71	−0.01	1.45	0.27	0.19
3	Prism RP	1.65	1.25	4.97	10.75	0.54	9.60	2.50	1.29	0.28	0.22
4	BetaMax Acid	1.89	1.54	7.15	17.40	0.70	7.90	9.54	1.40	0.34	0.24
5	Polaris C_{18} A	1.30	1.01	1.10	4.24	0.38	10.71	0.00	1.28	0.15	0.12
6	Polaris Amide C_{18}	1.67	1.40	11.79	36.91	0.67	9.31	2.39	1.50	0.23	0.15
7	MetaSil Basic	1.35	1.08	1.05	3.32	0.36	8.79	0.03	1.00	0.23	0.23
8	Synergi Polar-RP	1.35	1.07	0.75	2.37	0.20	8.72	−0.01	1.00	0.25	0.25
9	Symmetry C_8	1.18	1.05	1.08	4.97	0.38	9.31	0.16	1.00	0.18	0.18
10	Symmetry Shield RP8	1.43	1.19	1.13	2.05	0.54	9.47	0.08	1.39	0.28	0.20
11	HyPURITY C_8	1.21	1.00	0.80	3.80	0.37	9.17	0.00	1.00	0.19	0.19
12	HyPURITY Advance	1.80	1.30	5.25	6.85	0.76	6.98	3.81	1.44	0.50	0.35
13	Zorbax SB C_{18}	1.29	0.97	0.79	3.51	0.27	11.27	−0.01	1.00	0.12	0.12
14	Zorbax Bonus RP	1.73	1.34	6.29	16.93	0.53	11.08	1.17	1.33	0.27	0.20
15	Nucleosil C_{18} HD	1.23	1.00	0.79	3.90	0.33	10.87	0.00	1.00	0.12	0.12
16	Nucleosil Nautilus C_{18}	1.56	1.26	2.48	4.60	0.64	10.03	0.48	1.44	0.27	0.19
17	Discovery C_{18}	1.25	1.00	0.81	3.76	0.34	10.64	0.00	1.00	0.13	0.13
18	Discovery RP amide C_{16}	1.44	1.16	1.76	3.55	0.62	9.41	0.14	1.45	0.26	0.18
19	Purospher RP-18							3.04	1.00	0.13	0.13
20	Thermo BS535							13.35	1.00	0.20	0.20
21	Purospher RP-18e							0.01	1.00	0.10	0.10
22	Symmetry C_{18}							0.06	1.00	0.12	0.12
23	Symmetry Shield RP18	1.39	1.15	1.35	3.20	0.55	8.91	0.12	1.41	0.21	0.15
24	Polaris C_8 Ether							0.00	1.00	0.25	0.25
25	Polaris C_{18} Ether							0.00	1.00	0.14	0.14
26	HyPURITY Aquastar							−0.01	1.00	0.17	0.17
27	Atlantis dC_{18}							0.00	1.00	0.15	0.15
28	Suplex pKb										
29	Lichropsher RP Select B							0.00	1.00	0.24	0.24
30	Supelcosil ABZ	1.52	1.14	1.74	4.55	0.65	8.05				
31	Synergi Max RP	1.24	1.00	0.85	3.96	0.30	10.99				
32	XTerra MS18	1.27	1.00	0.82	3.66	0.31	11.26				
33	XTerra RP18	1.47	1.19	1.04	2.18	0.50	9.49				
34	HyPURITY C_{18}										
35	Acclaim PA C_{16}	1.46	1.2	1.91	4.54	0.47	8.66	0.11	1.45	0.21	0.15

Column no.	Column	Tanaka column characterisation protocol					
		k_{PB}	α_{CH_2}	$\alpha_{T/O}$	$\alpha_{C/P}$	$\alpha_{B/P}$ at pH 7.6	$\alpha_{B/P}$ at pH 2.7
1	XTerra MS C_8	1.15	1.30	0.87	0.42	0.33	0.10
2	XTerra RP8	1.10	1.26	1.73	0.30	0.17	0.07
3	Prism RP	2.54	1.33	1.66	0.38	0.59	0.01
4	Beta Max Acid	2.84	1.33	2.04	0.29	0.55	−0.03
5	Polaris C_{18} A	3.20	1.44	1.85	0.34	0.33	0.11
6	Polaris Amide C_{18}	2.87	1.43	2.43	0.20	0.15	−0.02
7	MetaSil Basic	2.03	1.32	1.25	0.32	0.29	0.09
8	Synergi Polar-RP	1.18	1.22	1.35	2.53	1.00	0.14
9	Symmetry C_8	3.47	1.38	0.95	0.39	0.40	0.02
10	Symmetry Shield RP8	2.30	1.32	1.87	0.27	0.19	0.04
11	HyPURITY C_8	1.59	1.35	1.00	0.34	0.30	0.11
12	HyPURITY Advance	1.13	1.00	1.59	0.39	0.80	0.13
13	Zorbax SB C_{18}	6.00	1.49	1.20	0.65	1.46	0.13
14	Zorbax Bonus RP	1.74	1.43	1.60	0.31	0.30	0.04
15	Nucleosil C_{18} HD	6.04	1.48	1.54	0.40	0.47	0.10
16	Nucleosil Nautilus C_{18}	3.37	1.40	1.98	0.33	0.48	0.01
17	Discovery C_{18}	3.32	1.48	1.51	0.39	0.28	0.10
18	Discovery RP amide C_{16}	1.65	1.35	1.81	0.49	0.44	0.19
19	Purospher RP-18	4.78	1.44	1.93	0.72	1.29	−0.07
20	Thermo BS535	1.35	1.36	2.71	0.67	0.86	−0.07
21	Purospher RP-18e	6.51	1.48	1.75	0.46	0.34	0.08
22	Symmetry C_{18}	6.51	1.46	1.49	0.41	0.68	0.01

Table 2 (*Continued*)

Column no.	Column	Tanaka column characterisation protocol					
		k_{PB}	α_{CH_2}	$\alpha_{T/O}$	$\alpha_{C/P}$	$\alpha_{B/P}$ at pH 7.6	$\alpha_{B/P}$ at pH 2.7
23	Symmetry Shield RP18	4.66	1.41	2.22	0.27	0.20	0.04
24	Polaris C_8 Ether	0.82	1.29	1.49	0.50	0.56	0.31
25	Polaris C_{18} Ether	2.98	1.45	1.63	0.46	0.38	0.10
26	HyPURITY Aquastar	1.32	1.39	2.65	1.25	2.66	0.13
27	Atlantis dC_{18}	3.74	1.45	1.23	0.61	0.56	0.11
28	Suplex pKb	1.24	1.35	2.84	0.34	0.29	0.00
29	Lichropsher RP Select B	2.76	1.32	1.21	0.66	1.40	0.14
30	Supelcosil ABZ	3.14	1.37	2.23	0.24	0.20	0.03
31	Synergi Max RP	4.91	1.44	1.15	0.33	0.32	0.08
32	XTerra MS 18	3.52	1.42	1.26	0.42	0.35	0.10
33	XTerra RP 18	2.38	1.29	1.83	0.33	0.20	0.07
34	HyPURITY C_{18}	3.20	1.47	1.60	0.37	0.29	0.10
35	Acclaim PA C_{16}	4.16	1.40	2.71	0.34	0.27	0.04

Column no.	Column	Modified partial Tanaka testing[a]					
		$\alpha_{B/P}$ at pH 7.6	$\alpha_{B/BA}$ at pH 7.6	$\alpha_{P/BA}$ at pH 7.6	$\alpha_{B/P}$ at pH 2.7	$\alpha_{B/BA}$ at pH 2.7	$\alpha_{P/BA}$ at pH 2.7
1	XTerra MS C_8						
2	XTerra RP8	0.13	0.18	1.45	0.07	0.10	1.46
3	Prism RP	0.58	0.78	1.33	0.00	0.00	1.34
4	BetaMax Acid	0.36	0.53	1.47	−0.04	−0.06	1.46
5	Polaris C_{18} A						
6	Polaris Amide C_{18}	0.18	0.26	1.49	0.00	0.00	1.51
7	MetaSil Basic						
8	Synergi Polar-RP						
9	Symmetry C_8						
10	Symmetry Shield RP8						
11	HyPURITY C_8						
12	HyPURITY Advance	0.36	0.54	1.50	−0.06	−0.10	1.52
13	Zorbax SB C_{18}						
14	Zorbax Bonus RP						
15	Nucleosil C_{18} HD	0.39	0.39	1.00	0.11	0.11	1.00
16	Nucleosil Nautilus C_{18}	0.52	0.78	1.50	0.04	0.06	1.53
17	Discovery C_{18}	0.39	0.39	0.98	0.11	0.11	1.00
18	Discovery RP amide C_{16}	0.26	0.36	1.42	0.06	0.09	1.44
19	Purospher RP-18						
20	Thermo BS535	0.86	0.93	1.08	−0.07	−0.07	1.08
21	Purospher RP-18e						
22	Symmetry C_{18}	0.43	0.42	0.98	0.05	0.05	1.00
23	Symmetry Shield RP18	0.24	0.32	1.36	0.03	0.04	1.41
24	Polaris C_8 Ether						
25	Polaris C_{18} Ether	0.56	0.60	1.07	0.16	0.17	1.08
26	HyPURITY Aquastar	2.08	1.89	0.91	0.12	0.13	1.13
27	Atlantis dC_{18}	0.40	0.38	0.94	0.12	0.12	0.96
28	Suplex pKb						
29	Lichropsher RP Select B						
30	Supelcosil ABZ						
31	Synergi Max RP						
32	XTerra MS18						
33	XTerra RP18						
34	HyPURITY C_{18}	0.37	0.37	1.00	0.11	0.11	1.00
35	Acclaim PA C_{16}	0.27	0.37	1.38	0.04	0.06	1.42

[a] Where possible the same column was used for the modified Tanaka as used in the standard protocol. Differences in the $\alpha_{B/P}$ results are attributed to differing batches of columns or as an "ageing" of the columns.

has been reported to be an amide-based polar embedded group [13], however it is not specified by ThermoElectron as such, whereas the Symmetry RP Shield C_8 possesses a carbamate polar group formed by a single stage bonding [4,20].

It can be concluded that the PC1–PC2 model for the 24 disparate phases describes over 90% of their chromatographic variability (see Fig. 4A and B). The PC1–PC2 score plot highlights that these phases can be categorised into four sub-groups (see Fig. 4A).

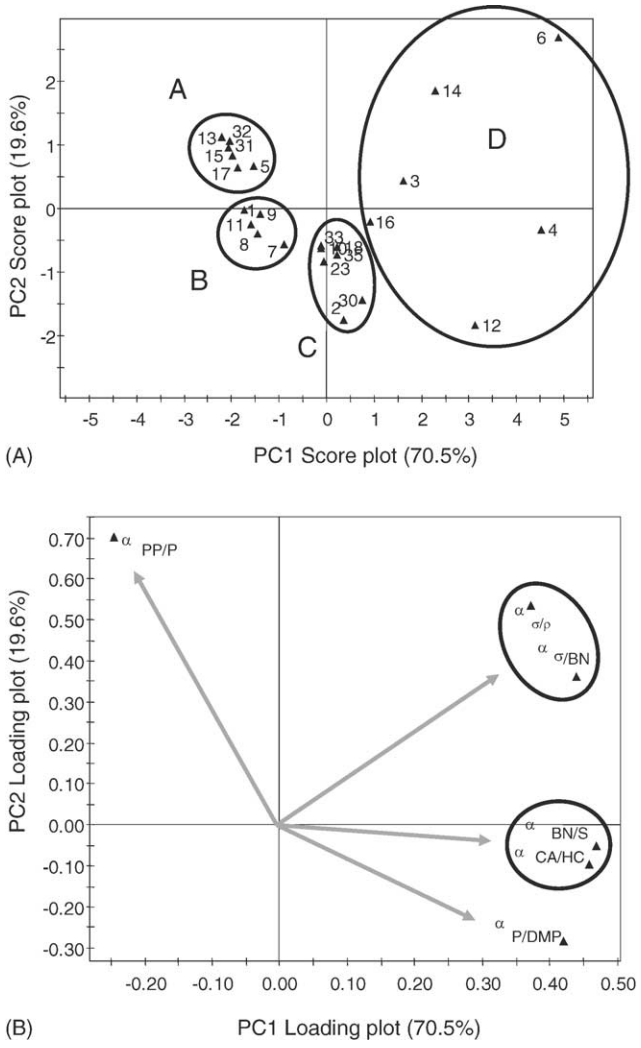

Fig. 4. PC1–PC2 plots for the acid mixture 1 evaluation: (A) score plot; (B) loading plot.

(i) Group A is a tight sub-grouping of phases containing alkyl phases with C_{12} and above ligands. Surprisingly this grouping contains the Polaris C_{18} A phase (column no. 5), which behaves more like a C_{18} phase than a PEG one as claimed by the manufacturer.

(ii) Group B is a cluster of C_8 or equivalent phases [i.e. the mixed alkyl phase MetaSil Basic (column 7) and the Synergi Polar RP which contains a phenyl ether moiety (column 8)].

(iii) Group C is a grouping of polar embedded phases many of which are known to be produced via a one-step bonding technology (i.e. Symmetry RP18, RP8 (columns 23 and 10, respectively) and XTerra RP18 and RP8 (columns 33 and 2, respectively) Shield phases from Waters). The other PEG phases in this cluster include the two amide phases from Supelco–Discovery RP Amide C_{16} and Supelcosil ABZ (columns 18 and 30, respectively) and the Acclaim PA C_{16} (column 35), which contains a sulphonamide and alkyl ether linkage. It is known that the Supelco phases are prepared via a two-step synthesis [26], however, any residual unreacted amino functionality is minimised by a further acylation step involving their reaction with a small acylating reagent (i.e. CH_3COCl).

(iv) Group D consisted of phases such as Polaris Amide C_{18} (column 6, amide), Zorbax Bonus (column 14, amide), Prism RP (column 3, urea), BetaMax Acid (column 4, not specified), HyPURITY Advance (column 12, believed to be an amide) and Nautilius C_{18} (column 16, not specified) that possess a wide variability in their chromatographic properties. The fact that they exhibit strong retention of 2-hydroxybenzoic acid compared to 4-hydroxybenzoic acid or benzoic acid suggests that these phases possess a high concentration of amino functionality presumably as a result of a two-step bonding technology.

The loading plot (see Fig. 4B) highlights that the groupings A–D (shown in Fig. 4A) possess the following dominant chromatographic properties:

(i) Group A: High hydrophobicity (positively correlated with the $\alpha_{PP/P}$ parameter), low shape/steric, low phenolic selectivity (negatively correlated with the $\alpha_{CA/HC}$, $\alpha_{BN/S}$ and $\alpha_{P/DMP}$ parameters) and low anionic selectivity (low $\alpha_{\sigma/BN}$ and $\alpha_{\sigma/\rho}$).

(ii) Group B: Moderate hydrophobicity, correlations as exhibited for group A.

(iii) Group C: Is located close to the origin highlighting that columns in this group do not correlate strongly with any of the parameters examined, i.e. they do not show a pronounced selectivity in any of the parameters examined.

(iv) Group D: High anion exchange capacity (positively correlated with the $\alpha_{\sigma/BN}$, $\alpha_{\sigma/\rho}$ parameters) moderate to high shape/steric and phenolic selectivity (positively correlated with the $\alpha_{CA/HC}$, $\alpha_{BN/S}$ and $\alpha_{P/DMP}$ parameters), low hydrophobicity (negatively correlated with the $\alpha_{PP/P}$ parameter).

These findings relating to Group D are in agreement with those of Neue [4,8,20,23], Layne [2] and Gruner [27] who observed that certain acidic analytes (i.e. maleic acid when analysed at pH 2.5 and 2-hydroxybenzoic acid at pH 3) exhibited enhanced retention on phases such as the Polaris Amide C_{18}. The presence of a residual positive charge on these phases is supported by the fact that they yield excellent peak shape and low retention of protonated basic analytes as a result of ionic repulsion [21]. As stated previously, the anion exchange functionality of the polar embedded phases may arise as a direct consequence of incomplete acylation of the aminopropyl silica of the phases prepared by the two-stage reaction.

The nitrogenous PEG phases (i.e. amide, urea, carbamate and sulphonamide phases) examined in this study exhibited enhanced retention of phenolic analytes as previously shown [23], in comparison, the ether-based PEG did not exhibit this phenolic selectivity.

The PC1–PC2 loading plot (Fig. 4B) also showed that the chromatographic parameters $\alpha_{CA/HC}$ and $\alpha_{BN/S}$ correlated suggesting that they measured the same shape/steric chromatographic property of the phase (to be discussed later). The anion exchange parameters $\alpha_{\sigma/BN}$, and $\alpha_{\sigma/\rho}$ also showed a moderate correlation. At the mobile phase pH of 2.5 (measured in the aqueous portion), it was assumed that all the acids would be in their unionized form, except for 2-hydroxybenzoic acid (pK_a = 3, approximately 24% ionized at pH 2.5). The latter analyte displayed considerable difference in retentivity depending on the stationary phase (the same affect was noted with the other acids on increasing the mobile phase to pH 3.5 and 4.5 and that the retention was as a function of the phosphate concentration) suggesting the enhanced retention was attributed to electrostatic interactions of the ionized acids with a positive charge on the phase.

The difference between a polar embedded phase and an alkyl phase bonded onto the same base silica can be clearly seen in the PCA contribution plot (see Fig. 5A and B) which shows that the PEG phases are less retentive (i.e. low $\alpha_{PP/P}$) and possess more shape/steric (i.e. $\alpha_{CA/HC}$ and $\alpha_{BN/S}$) and phenolic ($\alpha_{P/DMP}$) selectivity and, in the case of the HyPURITY Advance (see Fig. 5A), a high anion-exchange capacity (high $\alpha_{\sigma/BN}$ and $\alpha_{\sigma/\rho}$). In comparison, the contribution plots for the Symmetry Shield RP8 and the Symmetry C_8 (see Fig. 5B) exhibited the same differences as for the HyPURITY material except that the Symmetry Shield RP8 did not possess a lower retentivity—this was anomalous to all other PEG/alkyl column pairings. In addition, the Symmetry C_8 appeared to possess more anionic exchange capacity than the corresponding Shield material, which is prepared from a one-step reaction [4]. This is exactly in line with the recent findings of Mendez et al. [28] who showed that the Symmetry C_{18} material possessed anion exchange sites as a result of basic residues on the phase which arose from the bonding process—this may partially explain why the Symmetry C_8 and C_{18} phases exhibit such good peak shape for basic analytes (ionic repulsion) see reference [1].

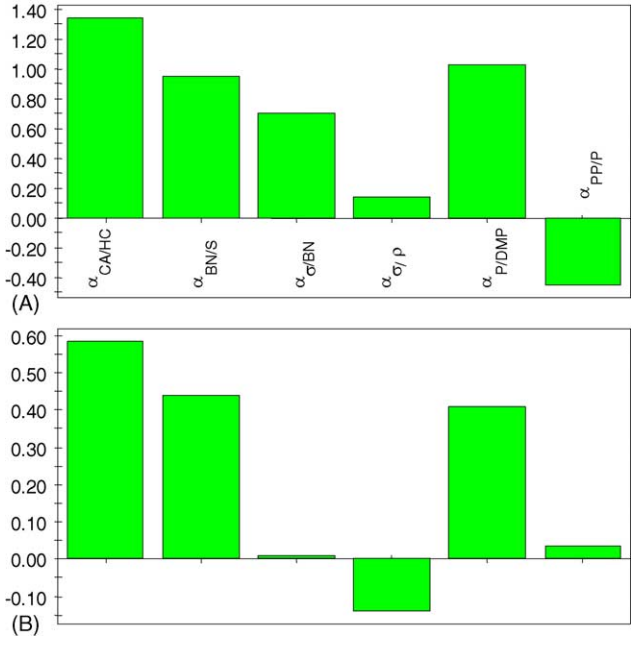

Fig. 5. Contribution plots: (A) HyPURITY Advance vs. HyPURITY C_8; (B) Symmetry RP8 Shield vs. Symmetry C_8.

3.3. Acid mixture 2

In order to compliment the previous tests and to rapidly assess the phenolic selectivity and anionic exchange capacity of a wide range of structurally dissimilar polar embedded phases, enhanced polar selectivity phases (often quoted has being polar endcapped) and to discriminate them from their corresponding alkyl analogues bonded onto the same base silica a new column characterization protocol was developed that utilized the analytes benzene sulphonic acid, toluene, phenol and benzylalcohol (see Fig. 2).

Thirty-one columns including 16 PEG, 9 alkyl, 2 Aqua phases with enhanced polar selectivity and 2 amino endcappped phases were characterized (see Table 2). A low ionic strength phosphate buffer (5 mM PO_4 pH 2.5 in MeOH–water, 65:35) was employed to maximise any ionic interactions of the stationary phase with the anionic analytes.

The selectivity factor of the fully ionized benzene sulphonic acid with the neutral marker toluene $\alpha_{BSA/TI}$ was shown to be a good indicator of the phase's degree of anionic character (i.e. the concentration of residual amino functionality). The $\alpha_{BSA/TI}$ value was <0.02 for the alkyl phases whereas for the PEG phases the value varied from 0 to 9.5 depending on the residual amino functionality of the phase. The nitrogenous PEG phases prepared from a single step reaction (i.e. XTerra RP, columns 2 and 33; Symmetry Shield RP, columns 10 and 23 and the Acclaim PA, column 35) and the non-nitrogenous PEG phases (i.e. Synergi Polar RP, column 8 and Polaris ether phases, columns 24 and 25) all generated low $\alpha_{BSA/TI}$ values. Phases such as the BetaMax Acid (column 4), Advance (column 12) and Zorbax Bonus RP (column 14) gave high $\alpha_{BSA/TI}$ values indicating considerable amino functionality possibly as a result of the incomplete acylation step in the two-stage reaction. The phenol/benzyl alcohol selectivity factor ($\alpha_{P/BA}$) demonstrated the phase's phenolic character (i.e. $\alpha_{P/BA} > 1.2$ highlighted phenolic selectivity) whereas the phenol/toluene selectivity factor ($\alpha_{P/TI}$) was far less discriminating. The selectivity between the two neutral markers benzylalcohol and toluene ($\alpha_{BA/TI}$) highlighted the phase's hydrophilicity.

PC1–PC2 for the dataset (see Table 2 and Fig. 6) explained over 80% of the variation; the standard alkyl, non-nitrogenous PEG and nitrogenous PEG phases which possessed a low anionic character lay on a straight line in the direction of the PC1 parameters—hydrophilicity $\alpha_{BA/TI}$, $\alpha_{P/TI}$. The hydrophilicity parameter $\alpha_{BA/TI}$, as expected, was inversely correlated ($r^2 = 0.80$, $n = 29$) to the Tanaka hydrophobicity term α_{CH_2}. Columns that lay on the line showed varying degrees of hydrophobicity, i.e. those on the left as typified by the Purospher

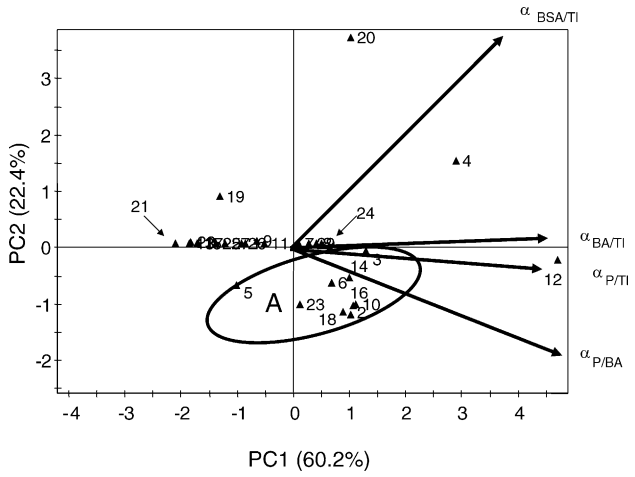

Fig. 6. Combined score and loading PC1–PC2 plots for the acid mixture 2 evaluation.

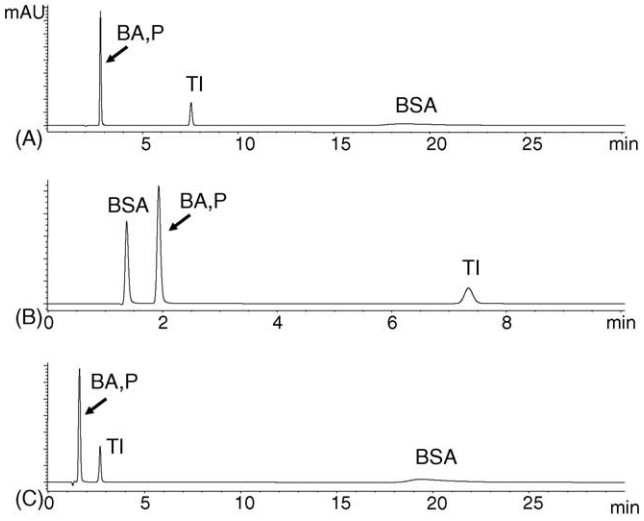

Fig. 7. Representative chromatograms of the acid mixture 2 using the phases: (A) Purospher RP18; (B) Purospher RP18e; (C) experimental amino end-capped phase Thermo BS535.

RP-18e phase (column no. 21) possessed low hydrophilicity whereas those on the right typified by the Polaris ether C_8 (column no. 24) possessed high hydrophilicity. It was interesting to note that the ether-based polar embedded groups (i.e. Synergi Polar-RP, column 8; Polaris C_{18} and C_8 ether phases, columns 24 and 25) behaved more like a standard alkyl phase in that they failed to exhibit any phenolic selectivity or anionic exchange capacity. The PEG phases possessing a low anionic character and high phenolic selectivity were located in sub-group A (see Fig. 6). There was a wide variation in chromatographic properties (i.e. hydrophilicity, phenolic selectivity and anionic character) of the remaining polar embedded phases (i.e. BetaMax Acid and Advance, columns 4 and 12, respectively) and the amino endcapped phase (Purospher RP18, column 19). The enhanced polar selectivity phases such as HyPURITY Aquastar and the Atlantis dC_{18} (columns 26 and 27, respectively) did not exhibit any enhanced phenolic selectivity. In contrast to the Purospher RP-18e phase (column 21), which lay on the straight line, the Purospher RP-18 phase (column 19) exhibited a marked anion-exchange capacity (i.e. $\alpha_{BSA/TI}$ value of 3.04 compared to 0.01 for the RP18e material). This was presumably due to the fact that the Purospher RP-18 phase possesses an amino endcapping [10,23] see Fig. 7A and B. In order to verify this, an experimental C_{18} phase with a high degree of endcapping with an amino functionality was examined (Thermo BS535, column 20). The phase was located in the polar embedded region of the PCA score plot (see Fig. 6) and chromatographically showed a high anionic exchange capacity as expected but no enhanced phenolic retention (see Fig. 7C).

3.4. Correlation of the combined Layne/Neue and the new anion-exchange/phenolic selectivity protocol with the Tanaka protocol

The Tanaka characterization protocol [22] is a well-established approach that has been favoured by many academic groups, stationary phase manufacturers such as ThermoElectron, Merck, Phenomenex, Macherey Nagel, Dionex and end users to assess and characterize stationary phases. The combined results of the testing described in this paper were correlated with the results obtained previously for identical stationary phases [21] and, where appropriate, new phases were characterized according to our previously published protocol (see Tables 1 and 2). The PC1–PC2 of this dataset is shown in Fig. 8A and B. The PC1–PC2 model describes nearly 70% of the chromatographic variability of the data. The PC1–PC2 score plot highlights that the 20 columns can be categorized into four well-defined sub sets as described in Fig. 8A. The loading plots (see Fig. 8B) show that the groupings are categorized by their following chromatographic properties:

(i) Group A standard C_{18} phases plus the Polaris C_{18} A are characterized by high hydrophobicity, low silanol activity, low shape/steric, low phenolic selectivity and low anion exchange capacity. The manufacturers of the Polaris C_{18} A phase (column 5) claim that it is a polar embedded phase, however, our results suggest that it may only contain a limited degree of amide functionality as it possesses a slightly higher steric and phenolic selectivity than for standard C_{18} phases.

(ii) Group B standard C_8 phases plus the phenyl ether phase (Synergi Polar-RP, column 8) and the mixed alkyl phase (MetaSil Basic, column 7) are characterized by moderate hydrophobicity, higher silanol activity, low shape/steric, low phenolic selectivity and low anion-exchange capacity.

(iii) Group C, containing the polar embedded phases with low anion exchange capacity, is characterized by a moderate hydrophobicity, high shape/steric and high phenolic selectivity.

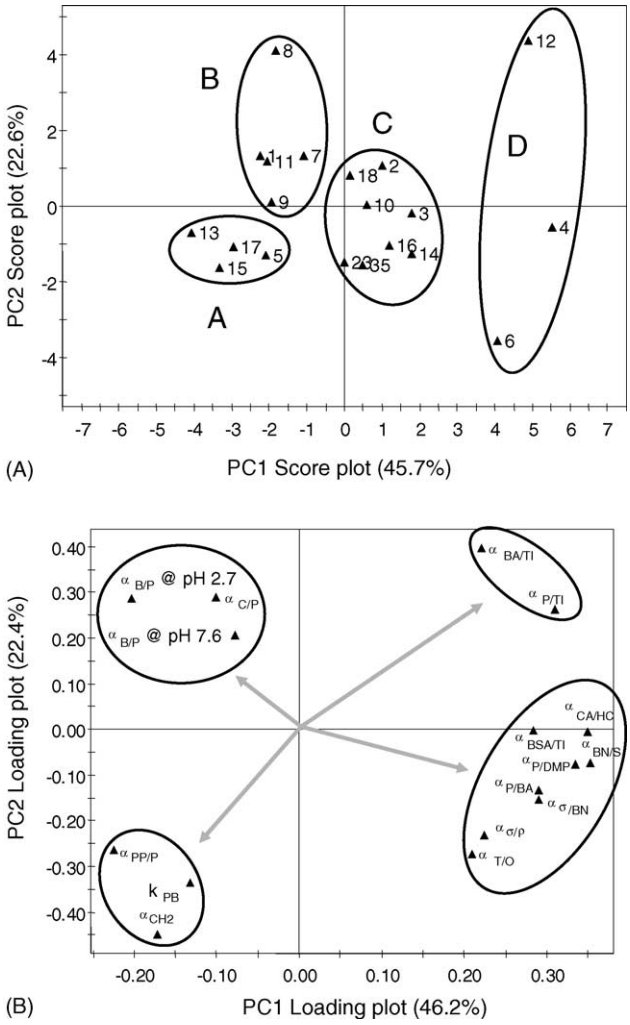

Fig. 8. PC1–PC2 plots for acid mixtures 1 and 2 and the Tanaka column characterization protocols: (A) score plot; (B) loading plot.

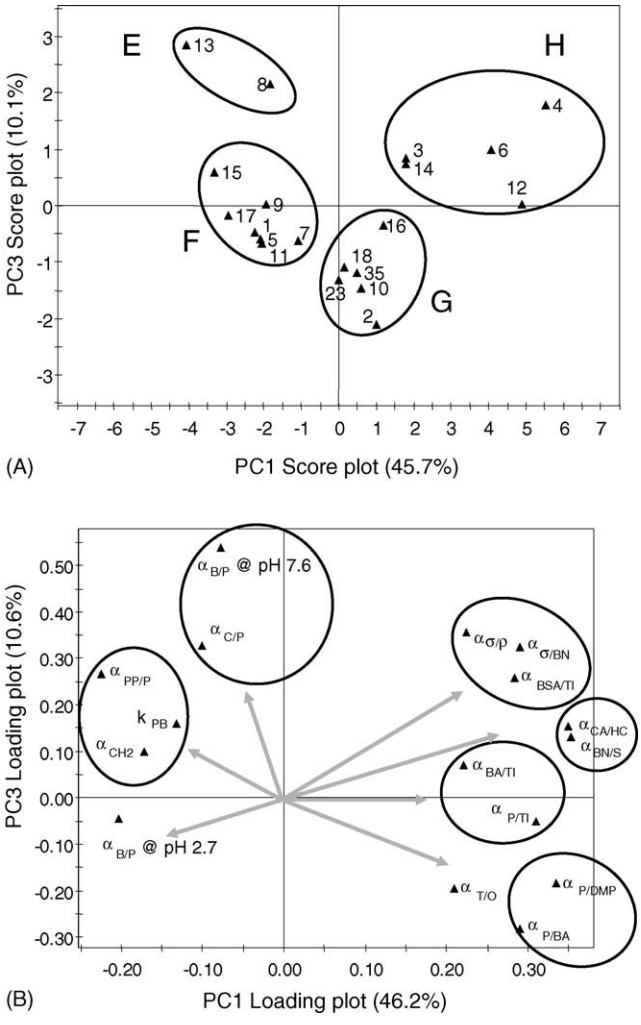

Fig. 9. PC1–PC3 plots for acid mixtures 1 and 2 and the Tanaka column characterization protocols: (A) score plot; (B) loading plot.

(iv) Group D contains polar embedded phases of widely differing chromatographic properties but all possess high anion-exchange capacity and high shape/steric and high phenolic selectivity.

The loading plot (Fig. 8B) highlighted that the following chromatographic parameters are correlated with one another—the hydrophobicity parameters $\alpha_{PP/P}$, k_{PB} and α_{CH_2} are positively correlated to one another and, as expected, negatively correlated to the hydrophilicity parameters $\alpha_{BA/Tl}$ and $\alpha_{P/Tl}$. The silanol/hydrogen bonding capacity parameters $\alpha_{B/P}$ at pH 2.7, $\alpha_{C/P}$, and $\alpha_{B/P}$ at pH 7.6 were positively correlated as previously shown [21]. The new shape/steric selectivity parameters $\alpha_{CA/HC}$ and $\alpha_{BN/S}$ correlated but did not correlate to the Tanaka shape/steric selectivity parameters $\alpha_{T/O}$. The phenolic selectivity parameters $\alpha_{P/DMP}$ and $\alpha_{P/BA}$ were observed to be correlated to one another. The anionic exchange capacity parameters $\alpha_{\sigma/BN}$, $\alpha_{BSA/Tl}$ and $\alpha_{\sigma/\rho}$ showed moderate correlation to each other.

Since the PC1–PC2 score plot only explained 69% of the variation, the PC1–PC3 plots were constructed and highlighted further differentiation of the phases (see Fig. 9A and B). The third PC contributed to 10% of the variability of the data. The standard alkyl phases with more silanol activity, such as the Zorbax SB C_{18} and the Synergi Polar-RP (columns 13 and 8) could be grouped together (Group E) as these possessed higher total silanol/hydrogen bonding activity. A group of low silanol activity alkyl phases were clustered together (Group F). The polar embedded phases could be separated into two groupings, those possessing low (columns 18, 23, 30, 10, 16 and 2) and high anion-exchange capacities (columns 4, 6, 12, 3 and 14) (Groups G and H, respectively). The loading plot (Fig. 9B) showed the same correlations as observed in the PC1–PC2 plot (Fig. 8B).

3.5. Phenolic selectivity using a modified Tanaka protocol

Due to the enhanced phenolic retention on nitrogenous containing polar embedded phases the Tanaka column characterization parameters $\alpha_{B/P}$ at pH 2.7, $\alpha_{C/P}$ and $\alpha_{B/P}$ at pH

7.6, which use phenol as their neutral marker, may be inappropriate for this class of phase. In order to assess this, 17 phases consisting of 10 polar embedded phases (i.e. carbamate, urea, amide, ether and sulphonamide moieties), four standard C_{18} phases, two "Aqua" phases and the experimental amino endcapped phase were chromatographed using the neutral marker benzylalcohol in addition to phenol. The results can be seen in Table 2.

The enhanced phenolic selectivity of the nitrogenous containing PEG phases such as the carbamate, amide, sulphonamide and urea-based phases could be easily detected from their $\alpha_{P/BA}$ parameter at either pH 2.6 or 7.6 which gave values >1.3. In comparison, no separation of phenol and benzylalcohol was observed on standard C_{18} phases (i.e. $\alpha_{P/BA} = 1$) using these chromatographic conditions. The more diverse amino endcapped, the two Aqua phases and the C_{18} ether, in contrast, exhibited marginal separation of the two components (i.e. $\alpha_{P/BA} = 1 \pm 0.1$).

The PC1–PC2 model for the 17 phases describes over 86% of the chromatographic variability within these phases (see Fig. 10A and B). The score plot (Fig. 10A) clearly highlighted two distinct groupings. Group A containing the standard C_{18} phases (plus the C_{18} ether, Atlantis dC_{18} "Aqua" phase) and Group B containing the experimental amino endcapped phase Thermo BS535 and the polar embedded phases, which possess a nitrogen atom in the polar moiety. There is a striking difference between the two "so-called" Aqua phases; from the loadings plot the HyPURITY Aquastar phase possesses a significantly higher silanol activity at pH 7.6 compared to the Atlantis dC_{18} phase (see Fig. 10A).

The fact that the original Tanaka silanol capacity parameters $\alpha_{B/P}$ at both pH 2.7 and 7.6 correlated with the new benzylamine/benzylalcohol parameter $\alpha_{B/BA}$ confirms the validity of using the former parameters (see Fig. 10B). However, it is strongly recommended that the Tanaka test protocol should be modified to incorporate benzylalcohol in the benzylamine/phenol test mixture in order to assess phenolic selectivity in the future.

3.6. Steric/shape selectivity parameters

The worthiness of various probes in order to assess steric/shape selectivity in RP chromatography has been much debated [21,29]. The probes that are used in the Tanaka protocol differ in their degree of planarity, i.e. the triphenylene is much more planar than the puckered σ-terphenyl molecule and as such, it has been suggested that triphenylene can slot in between the alkyl chains whereas with the puckered analyte this is less likely. Hence, triphenylene has a greater affinity for the C_{18} phase and elutes later than σ-terphenyl. We have previously [21] shown that the $\alpha_{T/O}$ value is larger for the nitrogen containing polar embedded groups ($\alpha_{T/O}$ value >1.8) compared to their corresponding alkyl phases ($\alpha_{T/O}$ value <1.5). If we compare the retention of triphenylene and σ-terphenyl by correcting for the column's hydrophobicity (as the polar embedded phases are inherently less retentive) by

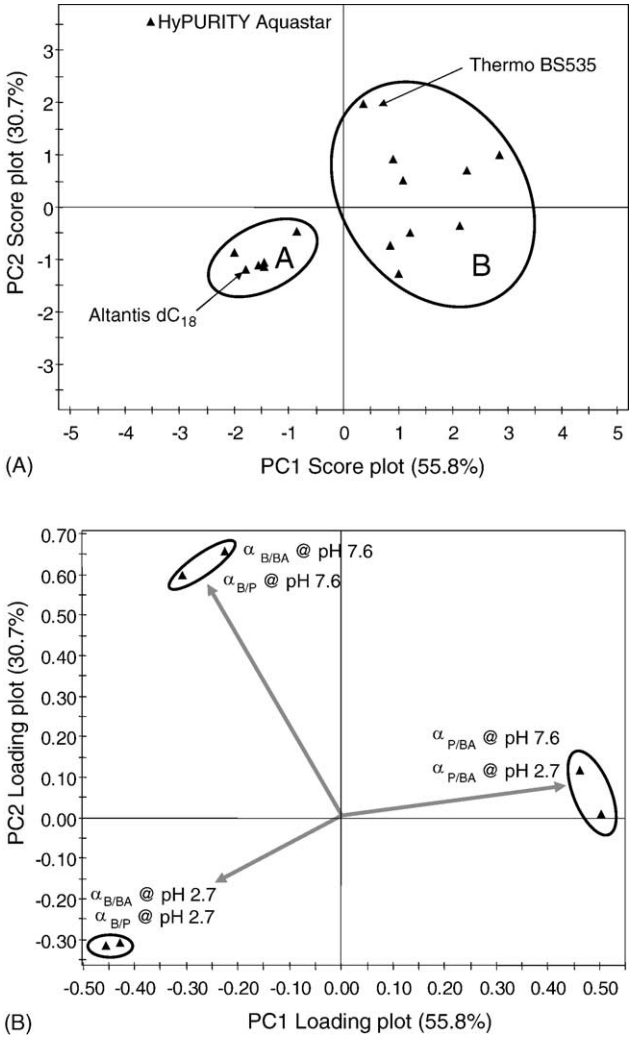

Fig. 10. PC1–PC2 plots for the modified Tanaka column characterization protocols: (A) score plot; (B) loading plot.

dividing the *k* values of the steric probes by the *k* value of the hydrophobic marker—*n*-pentylbenzene: it can be seen from Table 3 that it is the retention of the triphenylene analyte that increases rather than that of σ-terphenyl in the case of the polar embedded phases (as can be seen when one compares the $\alpha_{T/PB}$ and $\alpha_{O/PB}$ values). The $\alpha_{T/PB}$ value of the alkyl phases ranged from 0.88 to 1.54 whereas the value for the PEG phases ranged from 1.58 to 2.71. This implies that the insertion of a polar embedded group increases the "slot size" so that a greater portion of the triphenylene molecules can access the phase, whereas, the increase in size is not great enough to significantly alter the retention of the σ-terphenyl molecules. This is reflected in the effect of temperature on the $\alpha_{T/O}$ value for Symmetry C_8 and the Symmetry Shield RP8 materials (see Fig. 11). Lower temperatures were found to promote enhanced selectivity in the case of the polar embedded phase whereas no obvious improvement in selectivity was noted for the standard C_8 phase. At lower temperatures, the phase would be more rigid and hence it would exhibit a greater shape/steric selectivity supporting the use of temper-

Table 3
The Tanaka steric/shape retention and selectivity factors corrected for the phase hydrophobicity

Column no.	Column	k_{PB}	k_T	k_O	$\alpha_{T/PB}$	$\alpha_{O/PB}$	Ratio $\alpha_{T/PB}/\alpha_{O/PB}$
15	Nucleosil C_{18} HD	6.04	7.72	5.01	1.28	0.83	1.54
16	Nucleosil C_{18} Nautilis	3.37	6.24	3.16	1.85	0.94	1.97
9	Symmetry C_8	3.47	2.77	2.93	0.80	0.84	0.95
10	Symmetry Shield RP8	2.30	4.16	2.23	1.81	0.97	1.87
24	Polaris C_8 ether	0.82	1.23	0.83	1.50	1.01	1.48
25	Polaris C_{18} ether	2.98	4.36	2.68	1.46	0.90	1.63
7	MetaSil Basic	2.03	2.41	1.93	1.19	0.95	1.25
6	Polaris Amide C_{18}	2.87	6.17	2.54	2.15	0.89	2.43
5	Polaris C_{18} A	3.20	5.11	2.76	1.60	0.86	1.85
1	XTerra MSC_8	1.15	0.98	1.12	0.85	0.97	0.88
2	XTerra RP8	1.10	2.04	1.18	1.85	1.07	1.73
33	XTerra RP18	2.38	4.62	2.52	1.94	1.06	1.83
35	Acclaim PA C16	4.16	13.02	4.81	3.13	1.16	2.71
8	Synergi Polar RP	1.18	2.55	1.88	2.16	1.59	1.36
31	Synergi Max RP	4.91	4.85	4.20	0.99	0.86	1.15
11	HyPURITY C_8	1.59	1.34	1.34	0.84	0.84	1.00
34	HyPURITY C_{18}	3.06	4.07	2.57	1.33	0.84	1.58
32	XTerra MSC_{18}	3.52	3.55	2.83	1.01	0.80	1.25
14	Zorbax Bonus RP	1.74	4.19	2.62	2.41	1.51	1.60
23	Symmetry Shield RP18	4.66	9.74	4.38	2.09	0.94	2.22
18	Discovery RP amide C_{16}	1.65	2.90	1.60	1.76	0.97	1.81
17	Discovery C_{18}	3.32	4.25	2.81	1.28	0.85	1.51
4	BetaMax Acid	2.84	6.02	2.95	2.12	1.04	2.04
3	Prism RP	2.54	4.13	2.48	1.63	0.98	1.67

ature as a significant operating variable in method optimisation. As previously observed for other shape/steric probes [30] the selectivity factor for σ-terphenyl and triphenylene ($\alpha_{T/O}$) failed to be highly correlated with the cinnamic acid and 3-phenylpropionic acid ($\alpha_{CA/HC}$) and benzoic acid and sorbic acid ($\alpha_{BN/S}$) parameter ($r^2 > 0.5$). However, the latter two tests were observed to be highly correlated (i.e. $r^2 = 0.90$) with one another.

When one corrects the retention factor for cinnamic acid, 3-phenylpropionic acid, benzoic acid and sorbic acid for the hydrophobicity of the phase (i.e. divide the *k* of the analyte by the *k* of the neutral marker dimethylphthalate) it is apparent that it is the analytes cinnamic and benzoic acid that are retained longer on the polar embedded phases than on the corresponding alkyl phases (see Table 4) and to a greater extent than 3-phenylpropionic acid and sorbic acid. There

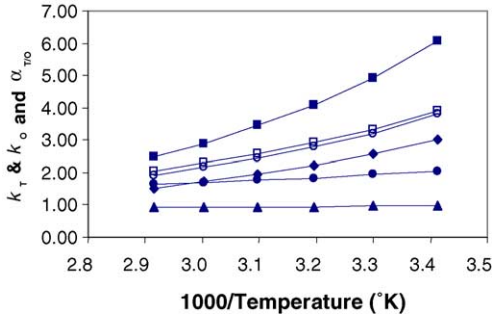

Fig. 11. Retention factor vs. the reciprocal of temperature. Key: (■) k_T on Symmetry RP8 Shield; (□) k_O on Symmetry C_8; (◯) k_T on Symmetry C_8; (♦) k_O on Symmetry RP8 Shield; (●) $\alpha_{T/O}$ on Symmetry RP8 Shield; (▲) $\alpha_{T/O}$ on Symmetry C_8.

was an excellent correlation between $\alpha_{BN/DMP}$ and $\alpha_{CA/DMP}$ ($r^2 = 0.99$) and $\alpha_{S/DMP}$ and $\alpha_{HC/DMP}$ ($r^2 = 0.93$) selectivity parameters.

From the three shape/steric parameters used in this study, the probes cinnamic acid, benzoic acid and triphenylene are

Table 4
The acid mixtures 1 and 2 steric/shape selectivity factor corrected for the phase hydrophobicity

Column no.	Phase	$\alpha_{C/DMP}$	$\alpha_{HC/DMP}$	$\alpha_{BN/DMP}$	$\alpha_{S/DMP}$
5	Polaris C_{18} A	1.74	1.34	0.71	0.71
6	Polaris Amide C_{18}	3.34	2.00	1.54	1.10
13	Zorbax SBC_{18}	1.40	1.09	0.57	0.58
14	Zorbax Bonus RP	3.17	1.83	1.44	1.07
9	Symmetry C_8	1.61	1.37	0.71	0.68
10	Symmetry Shield RP8	1.94	1.35	0.88	0.74
7	MetaSil Basic	1.55	1.15	0.70	0.65
23	Symmetry Shield RP18	2.00	1.44	0.87	0.76
1	XTerra MS8	1.27	1.00	0.58	0.58
2	XTerra RP8	1.81	1.23	0.83	0.70
30	Supelcosil LC-ABZ	2.41	1.59	1.05	0.93
32	XTerra MS18	1.52	1.19	0.61	0.61
33	XTerra RP18	1.87	1.27	0.82	0.69
8	Synergi Polar RP	0.93	0.69	0.36	0.34
31	Synergi Max RP	1.44	1.16	0.58	0.58
15	Nucleosil C_{18} HD	1.61	1.31	0.65	0.65
16	Nucleosil C_{18} Nautilius	2.66	1.70	1.21	0.95
17	Discovery C_{18}	1.65	1.31	0.66	0.66
18	Discovery Amide C_{16}	2.30	1.59	1.02	0.88
11	HyPURITY C_8	1.58	1.30	0.69	0.69
12	HyPURITY Advance	2.84	1.58	1.43	1.09
3	Prism RP	2.54	1.54	1.17	0.94
4	BetaMax Acid	4.12	2.18	2.02	1.32

Table 5
Molecular properties of the steric/shape selectivity probes

Molecule name	Dipole moment (1)	Molecule volume (2)	Total surface area (3)	log D at 2.5 (4)
Sorbic acid (S)	2.49	186.08	159.05	1.34
Benzoic acid (BN)	2.34	185.01	144.61	1.89
Phenylpropronic acid (HC)	3.15	252.55	189.73	1.84
Trans-cinnamic acid (CA)	3.13	235.13	181.59	2.39
σ-Terphenyl (O)	1.25	409.68	270.27	5.30
Triphenylene (T)	0.99	392.26	241.73	5.90

Molecular descriptors (1–3) calculated using an AstraZeneca in-house programme. Descriptor 1: topical dipole moment; descriptors 2 and 3: van der Waals radius-based volume and total surface area, respectively; Descriptor 4: log D at pH 2.5 calculated using ACD software.

retained to a greater extent compared to their counterparts 3-phenylpropanoic acid, sorbic acid and σ-terphenyl on the polar embedded phases. A rationale for this chromatographic behaviour may lie in the fact that the latter probes possess a larger total surface area and molecule volume than the former ones (see Table 5), i.e. the bigger the molecule, the more difficulty it has in penetrating into the alkyl layer and hence it will not be retained to the same extent as a smaller molecule. Simple molecule modelling of the nitrogen containing phases compared to a straight alkyl phase suggests that the former phase possesses a much more open architecture in which the smaller probes can penetrate, the elution order on the PEG phases mirrors closely the log D of the molecules at pH 2.5 (see Table 5) suggesting that the retention is primarily dominated by partitioning rather than by an additional secondary retention mechanism.

4. Conclusion

The modified column characterization protocols by Layne, Waters and Tanaka, when combined with the chemometrical tool of PCA, have been shown to be a powerful and easy way of discriminating between commercially available PEG phases, standard C-alkyl and amino endcapped phases. It is paramount that chromatographers obtain a better understanding of the differences in chromatographic properties between these generically termed PEG phases—as, in general, stationary phase manufacturers are extremely unwilling to divulge the exact bonding chemistry employed. A better understanding of these PEG phases will undoubtedly enable chromatographers to exploit the properties of these phases more fully, to minimise any of their undesirable properties and to greatly assist in rational column selection.

The wide chromatographic differences observed between the PEG phases observed in the PCA can be explained in terms of the bonding chemistry/technology employed, for example, one and two stage synthesised nitrogen containing PEG phases can be easily distinguished from one another; also the ether-based PEG phases did not exhibit any phenolic or anionic exchange character.

The study has also identified anionic sites on a number of standard C-alkyl phases, this is due to deliberate incorporation of amino endcapping by the stationary phase manufacturers or from residual traces of amino catalysts trapped within the matrix of the phase, this may account for the excellent peak shape of these phases for the analysis of basic analytes whereas peak symmetry may be poor for the analysis of ionized acids.

The PCA loading plots for the correlation of the column characterization protocols evaluated in this study have shown that many of the parameters correlate with one another; therefore it is possible to simplify the number of tests performed on each column to fully characterize it. One such approach would be to standardise on the Tanaka protocol with the addition of the following tests—anion exchange parameter ($\alpha_{BSA/Tl}$), phenolic selectvity ($\alpha_{P/BA}$) and possibly an extra shape/steric term ($\alpha_{BN/S}$). From this work, it is highly recommended that this approach be adopted in future column characterization protocols when diverse phases are being examined.

Acknowledgements

The authors wish to thank the many stationary phase manufacturers, column suppliers for providing new columns, ThermoElectron for providing the experimental amino endcapped phase for this study and Mr. Richard Lunn for providing technical support to the early part of this work.

References

[1] J.E. O'Gara, D.P. Walsh, C.H. Phoebe Jr., B.A. Alden, E.S.P. Bouvier, P.C. Iraneta, M. Capparella, T.H. Walters, LC–GC North Am. 19 (2001) 632.
[2] J. Layne, J. Chromatogr. A 957 (2002) 149.
[3] D.V. McCalley, J. Chromatogr. A 844 (1999) 23.
[4] J. O'Gara, B. Alden, T. Walter, J. Petersen, C. Niederländer, U. Neue, Anal. Chem. 67 (1995) 3809.
[5] H. Engelhardt, D. Mathes, J. Chromatogr. 142 (1977) 311.
[6] H. Engelhardt, D. Mathes, J. Chromatogr. 185 (1979) 305.
[7] H. Engelhardt, G. Ahr, M.T.W. Hearn, J. Liq. Chromatogr. 4 (1981) 1361.
[8] U.D. Neue, Y.-F. Cheng, Z. Lu, B.A. Alden, P.C. Iraneta, C.H. Phoebe, K. Van Tran, Chromatographia 54 (2001) 169.
[9] U.D. Neue, B.A. Alden, T.H. Walter, J. Chromatogr. A 849 (1999) 101.
[10] Á. Sandi, L. Szepesy, J. Chromatogr. A 818 (1998) 1.
[11] Á. Sandi, L. Szepesy, J. Chromatogr. A 818 (1998) 19.

[12] Á. Sandi, L. Szepesy, J. Chromatogr. A 845 (1998) 113.
[13] N.S. Wilson, J. Gilroy, J.W. Dolan, L.R. Snyder, J. Chromatogr. A 1026 (2004) 91.
[14] T.S. Reid, R.A. Henry, Am. Lab. 31 (1999) 24.
[15] R.E. Majors, M. Przybyciel, LC–GC Eur. 15 (2002) 2.
[16] B. Buszewski, J. Schmid, K. Albert, E. Bayer, J. Chromatogr. 552 (1991) 415.
[17] T.L. Ascah, B. Feibush, J. Chromatogr. 506 (1990) 357.
[18] T.L. Ascah, K.M.R. Kallury, C.A. Szafranski, S.D. Corman, F. Liu, J. Liq. Chromatogr. Relat. Technol. 19 (1976) 3049.
[19] T. Czajkowska, I. Hrabovsky, B. Buszewki, R.K. Gilpin, M. Jaroniec, J. Chromatogr. A 691 (1995) 217.
[20] J.E. O'Gara, D.P. Walsh, B.A. Alden, P. Casellini, T.H. Walter, Anal. Chem. 71 (1999) 2992.
[21] M.R. Euerby, P. Petersson, J. Chromatogr. A 994 (2003) 13.
[22] K. Kimata, K. Iwaguchi, S. Onishi, K. Jinno, R. Eksteen, K. Hosoya, M. Arki, N. Tanaka, J. Chromatogr. Sci. 27 (1987) 721.
[23] U.D. Neue, K. Van Tran, P.C. Iraneta, B.A. Alden, J. Sep. Sci. 26 (2003) 174.
[24] H. Engelhardt, R. Grüner, M. Scherer, Chromatographia 53 (2001) 154.
[25] T. Czajkowska, M. Jaroniec, J. Chromatogr. A 762 (1997) 147.
[26] Pharm. Forum 29 (2003) 170.
[27] R. Grüner, H. Engelhardt, Presented at the 22nd International Symposium on Chromatography, Rome, 1998.
[28] A. Méndez, E. Bosch, M. Rosés, U.D. Neue, J. Chromatogr. A 986 (2003) 33.
[29] N.S. Wilson, J.W. Dolan, L.R. Snyder, P.W. Carr, L.C. Sander, J. Chromatogr. A 961 (2002) 217.
[30] M.R. Euerby, D. Hassey, P. Petersson, J.W. Dolan, L.R. Snyder, Presented at the 26th International Symposium on HPLC Separations and Related Techniques, Montreal, 2002.
[31] R.J.M. Vervoort, A.J.J. Debets, H.A. Claessens, C.A. Cramers, G.J. de Jong, J. Chromatogr. A 897 (2000) 1.
[32] D. Visky, Y. Vander Heyden, T. Iványi, P. Baten, J. De Beer, Z. Kovács, B. Noszál, E. Roets, D.L. Massart, J. Hoogmartens, J. Chromatogr. A 977 (2002) 39.
[33] H.A. Claessens, M.A. van Straten, C.A. Cramers, M. Jezierska, B. Buszewski, J. Chromatogr. A 826 (1998) 135.
[34] H. Engelhardt, H. Lőw, W. Gőtzinger, J. Chromatogr. 544 (1991) 371.
[35] R.G. Brereton, D.V. McCalley, Analyst 123 (1998) 1175.